Journal of Innovative Image Processing (ISSN: 2582-4252)
www.irojournals.com/iroiip/

Radio thermal Dual-Imaging Fusion Network for Deep Feature-Driven Breast Cancer Detection

Suriya K.[1], Praveen Kumar R.[2], Nithyashree V.[3], Dhanusri S.[4], Abinaya K.[5], Ranjana A.[6]

Department of Electronics and Communication, Easwari Engineering College, Anna University, Chennai, India.

E-mail: [1]nithisuriya@gmail.com, [2]rpjcspraveen@gmail.com, [3]nithyashreevenkatesan2@gmail.com, [4]sdhanusri225@gmail.com, [5]abitwinklex.345@gmail.com, [6]rannjanaarun@gmail.com

Abstract

Breast cancer is one of the major problems affecting the breast that is very commonly detected in females, and it requires efficient and precise diagnosis for enhanced stages of survival. To achieve efficient, precise, and contactless diagnostic processes, it is proposed that the Radio Thermal Dual-Imaging Fusion Framework be utilized in combination with the structural information obtained from mammogram images, along with thermal information obtained from infrared images of thermograms of the breasts. This paper proposes a conceptual design that makes use of an available set of mammogram images taken from digital image databases, such as The Mammographic Image Analysis Society Database (MIAS), standard sets of samples from the curated Breast Imaging Subset of the Digital Database for Screening Mammography (CBIS-DDSM), as well as samples from anonymized patients in recent routine clinical screenings, similar to recent diagnostic studies that utilized mammography. The samples for thermal images were obtained from infrared images of thermograms of breasts, which are still very much in use in today's breast cancer diagnostic research. The proposed conceptual design for diagnosis will employ the Super-Fast Recurrent Convolutional Neural Network (SFRCNN) architecture, which will be a ResNet-50 based architecture for the extraction of thermal images and standard images, as mentioned above. The preprocessing for sampling the modalities will be done using grayscale normalization of the standard mammogram images as well as standard thermal mapping for the infrared images. From the results of the proposed conceptual design, it has been identified that the proposed dual-imaging modality accuracy of 84.75% will be obtained by using the standard mammogram images and the standard infrared images, representing a significant improvement over standard image processing, as an improvement in accuracy of 3% is expected from the proposed standard approaches within the benchmark design for the Convolutional Neural Network model due to the proposed dual-imaging modality technique, along with a proposed diagnosis accuracy for assessing a sensitivity of 98.04% by the dual-imaging modalities of the standard infrared images.

Keywords: Mammogram, Thermogram, Image Processing, Medical Images, Breast Cancer.

DOI: https://doi.org/10.36548/jiip.2025.4.020
Received: 07.11.2025, received in revised form: 06.12.2025, accepted: 20.12.2025, published: 31.12.2025

1. Introduction

Breast cancer is among the most widespread cancer cases, affecting women from all over the world, and is also one of the major causes of cancer-related deaths [2]. The early detection of different cases of cancer is especially significant for patients with breast cancer, as it can help them receive much better treatment and extend their lifespan. As stated in global health news, breast cancer is one of the most commonly diagnosed cancers each year worldwide, particularly among females. Genetic factors, hormonal factors, and lifestyle factors also influence the incidence of breast cancer. The influence of hormone levels, previous pregnancy complications, and high sensitivity to estrogen are just a few factors that increase the likelihood of developing breast cancer [1]. In medical practice, most females who exhibit observable symptoms and irregularities are initially examined by ultrasound and other technologies supervised by radiologists. Various technologies can be applied to examine and assess cases of breast cancer, especially during their early stages. The most widely used method for examining and detecting breast cancer, particularly in its early stages, is still mammography. It should be noted that not all breast lesions discovered are cancerous; many indicate other health problems that require precise differentiation [4]. Different medications and therapies for hormone imbalances can also increase the risk of developing breast cancer, so they should be closely monitored by doctors. Mammography is one of the most significant diagnostic tools used during examinations to detect breast cancer in its early stages. The early detection of breast cancer significantly enhances treatment options and enables affected females to live longer. If not discovered and treated in time, cases of breast cancer can worsen and spread to other parts of the body via lymph nodes. Computer-aided diagnostic tools assist doctors in identifying and analyzing abnormal cases of breast cancer during various examinations. The testing and examination of breast cancer cases involve conducting various medical tests and procedures that aid in providing an accurate diagnosis. Recent advances in machine learning, artificial intelligence, and image analysis techniques have made it easier for computers to accurately detect breast anomalies. The new edge-AI technology also facilitates fast image data analysis and early breast cancer diagnosis due to quicker image data processing. Thus, breast cancer diagnosis has gradually shifted from manual interpretation to machine learning-based diagnostic processes.

1.1 Role of Cancer Segmentation in Mammogram Images

Segmentation is an essential process in the analysis of mammography images because it allows for the separation of the region of interest from the surrounding biological structures. The analysis of mammograms can sometimes be complicated when mammographic densities make the boundaries of lesions hard to define. The process of segmentation can facilitate the separation of areas of potential malignancy from the surrounding breast tissue.

In clinical image analysis, it is observed that mammographic images have different types of noise or artefacts, which depend on various image acquisition and patient anatomical features. Pre-processing techniques, such as median filtering and intensity adjustment, are used to eliminate unwanted variability in the image to enhance its analytical features. It should be noted that as noise and intensity in an image are decreased, there is an increased possibility of finding appropriate features in early-stage abnormalities. Different strategies have also emerged for segmenting mammographic features in an image, ranging from simple thresholding to advanced edge and/or region-based segmentation. However, classical models, although useful in some applications, tend to be inefficient when there is an irregular boundary

of the lesion and inhomogeneous tissue density in the image. These difficulties have initiated a significant increase in interest in developing models that adapt better to the features of different image qualities and tissue patterns.

Machine learning, and more recently deep learning toolkits, have enjoyed widespread use in breast image segmentation tasks due to their unique ability to learn patterns from sample images, as opposed to traditional approaches that focus on handpicked features. Deep-learning models have proven particularly effective for grayscale mammograms because of their ability to handle intensity differences within an image that can indicate tumors. Although manual annotation by radiologists is still regarded as the gold-standard methodology, its increasing complexity due to a higher number of screening studies renders full manual segmentation unfeasible.

Though mammography basically entails structural information, in this study, thermal images are also taken into consideration to provide a combination of anatomical details with surface temperature patterns. By doing this, the framework can benefit from both structural and physiological information while localizing a lesion, which could be more helpful when purely structural information is not enough [18].

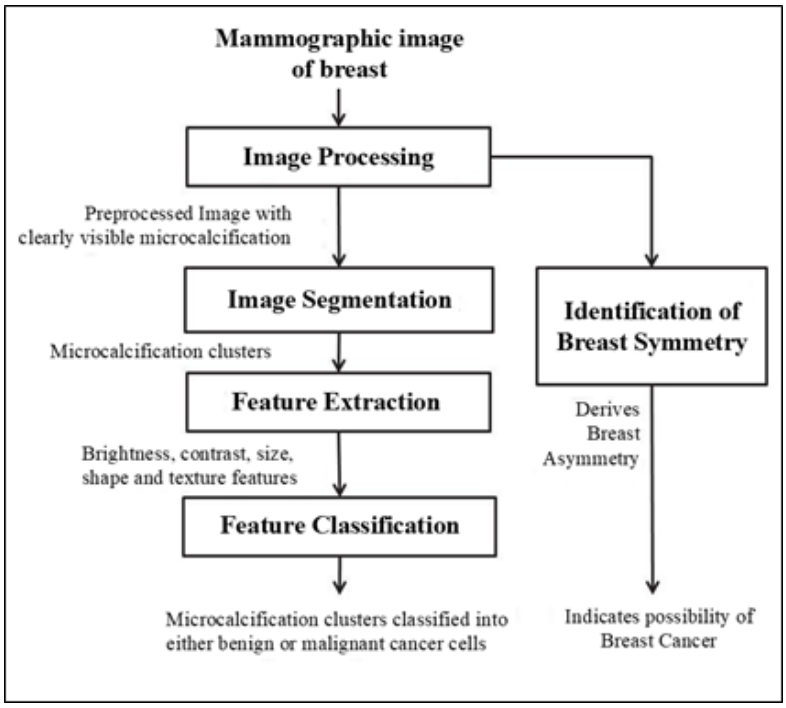

Figure 1. The Overall Process Involved in the Detection of Breast Cancer

Thermal imaging is also commonly employed for the study of the variation in the surface temperatures of the breast region, and these temperatures can provide indications of the regions that may be irregular. Contrary to other diagnostic methods that may be invasive, thermography provides information on the distribution of heat materialized on the outer layers and the behavior of the blood vessels beneath the breast region. The growth of tumors is commonly associated with the heightened activity of the vessels, indicated by the warm regions apparent on the thermogram. This study will provide input for the analysis of the mammographic images alongside the thermal images, such that the combinations of structural information and thermal information will be taken into consideration.

Figure 1 illustrates the general sequence in cancer-related image analysis. This entails the reading and processing of the mammogram image, followed by segmentation, where the breast part of the image is distinguished from the rest of the image, including any part that could require further analysis. This region is then evaluated using a variety of feature measurements chosen depending on how it can be described in terms of its characteristics, which are essentially qualities of size, contrast, intensity, and texture. These factors provide a platform for determining whether it is a malignant or benign instance.

To analyze the efficiency of the proposed system, a super-fast recurrent CNN-based deep learning approach has been considered. The proposed system operates by leveraging a series of convolutional layers to analyze the deeper patterns within the image. Consequently, the approach is able to provide a more detailed interpretation of the medical images by focusing on the deeper image patterns, which are not considered by other simple networks. The research also takes into consideration the limitations highlighted in previous research works. Many of the approaches used in previous research have confronted the challenges of delays in processing time, complex structures of the models, and difficulty in obtaining important features through the use of basic approaches or approaches based on fuzzy logic.

The rest of the paper is organized in the following way: Section 2 discusses the background information. Thermal imaging is also commonly employed for the study of the variation in the surface temperatures of the breast region, and these temperatures can provide indications of the regions that may be irregular. Contrary to other diagnostic methods that may be invasive, thermography provides information on the distribution of heat materialized on the outer layers and the behavior of the blood vessels beneath the breast region. The growth of tumors is commonly associated with the heightened activity of the vessels, indicated by the warm regions apparent on the thermogram. This study will provide input for the analysis of mammographic images alongside thermal images, such that the combinations of structural information and thermal information will be taken into consideration.

2. Related Work

Dabass et al. [7] introduced a framework for breast-cancer detection in ultrasound images by identifying the region of interest. Their study highlighted several practical difficulties associated with ultrasound imaging, including motion artefacts, variable contrast, and significant noise levels. These issues often slow down the decision-making process and reduce the visibility of finer structures. Since the images require several rounds of filtering to suppress noise, the overall resolution is affected, and the segmentation output becomes less reliable for subsequent classification tasks.

Ibrahim et al. [8] proposed a Chaotic Swarm Search Algorithm (CSSA) for segmenting thermal images of the breast. While the method attempts to refine superpixel boundaries and enhance tumor visibility through chaotic map functions, the algorithm suffers from slow convergence and a tendency to stagnate at local optima. A key limitation noted by the authors is that thermal images are inherently two-dimensional, whereas the optimization process treats most parameters as one-dimensional values. This mismatch affects the quality of image matching and degrades segmentation accuracy. Their work suggests that future improvements may require a shift toward deep-learning-based architectures.

Robin et al. [9] presented a neural-network-based system for tumor-region identification using mammographic images. The framework employed a convolutional

architecture to analyze multiple feature patterns and used histopathological information to validate the segmentation results. However, the authors observed that when the input dataset contains limited or low-quality features, the model struggles to generalize and the classification performance decreases. They emphasized the need for image-focused model selection and improved feature extraction to overcome this challenge.

Khasana et al. [10] explored a watershed-based segmentation method combined with thresholding to detect cancer-affected regions using hospital imaging data. Their system reported a detection accuracy of 88.65%, and the comparative study with other state-of-the-art approaches showed its potential for clinical use. Nonetheless, the watershed technique is highly sensitive to variations in image resolution; when the gray-level distribution differs across scans, the threshold selection becomes inconsistent and affects the classification outcome. Several recent studies have also investigated the role of image enhancement and preprocessing in improving mammogram-based computer-aided diagnosis systems [21], [22].

Nguyen et al. [11] investigated the use of fuzzy-logic-based probability distribution techniques for analyzing mammographic images. Regions of interest were isolated by evaluating the pixel distributions through the histogram and the gray-level segmentation. Although their approach was able to separate the normal and abnormal cases to some extent, it relies on a limited range of pixel-intensity information. Because mammograms often contain multiple intensity levels that carry diagnostic significance, extracting only a narrow band of these levels is insufficient for dependable cancer assessment.

Georgas et al. [12] examined mammographic and MRI data for early breast cancer detection and proposed a Rad-Efficient Network using a pipelined CNN architecture. Their dataset consisted of 104 cases (45 benign and 59 malignant), and the model achieved an accuracy of 82%. The study noted that combining the radiomic features from the different modalities is complex, and the integration process can restrict the overall learning capacity of the model, particularly when handling the varied breast-lesion characteristics.

A range of additional studies has also contributed to the development of breast cancer detection frameworks using deep learning and machine learning. These works explored issues such as feature-extraction limitations, segmentation precision, classification reliability, and model optimization strategies [13], [14]. Collectively, the existing literature highlights the need for more adaptable models capable of handling multimodal data and providing stable performance across diverse imaging conditions.

3. Proposed Work

The research work in the current context attempts to merge two different sources of imaging information: mammogram images and breast thermogram images—to create a single system capable of analyzing both types of structural information as well as temperature-based information. The logic behind using these two different types of imaging information lies in the fact that each represents a different type of data. Mammogram images provide insight into the inner structure of breast tissues, whereas thermogram images capture the surface heat patterns associated with changes in the blood vessels. The idea is to process the two types of information separately at the beginning and then analyze the collective knowledge provided by both streams of information to easily identify signs of potential abnormalities, which are much more accurate in terms of early detection compared to existing individual systems. The proposed approach consists of the overall design of the procedure, starting with the preparation

of the datasets of images and the identification of the technical challenges that exist in the context of processing these images. The model then employs a carefully selected set of approaches to implement the two types of images effectively, enabling the analysis and combination of the information in a manner that facilitates accurate classification. The next section delves into more detail regarding the proposed approach.

3.1 Data Collection

In this study, two separate sets of data were used for breast image analysis. These included a collection of mammography images in normal scan format, which were further categorized as infrared thermograms. These two sets were found to hold exactly five hundred images in each case. Based on initial checks for a suitable mammography image source, it appears that a large number of images were sourced from a public Kaggle dataset with reference to the "Mammographic Image Analysis Society (MIAS) database." In addition to this, another public resource used for mammography image analysis has been referred to, which appears to be the "Curated Breast Imaging Subset of the Digital Database for Screening Mammography (CBIS-DDSM)". These mammograms were normal grayscale images with a non-uniform resolution in terms of pixels, which varied between 512×512 pixels and a maximum of 1024×1024 pixels in size.

The thermogram images used here have been derived from the infrared breast thermography database, which has been used by many researchers for recent works on detecting breast cancer using the CNN technique [19], [17]. The thermogram images were produced in controlled environments and are representative of the manner in which heat distribution occurs in the breast area. In some of the thermogram images, regions of slightly warmer areas are more visible than other areas. Such phenomena are typically representative of blood flow and other metabolic processes.

Before attempting to analyze, each color thermogram was unified to a single-channel thermal image to ensure that the data came in a standardized form. After this was achieved, each image, whether mammography images or thermograms, was resized to 256×256 pixels to conform to the input requirement demanded in the subsequent steps of the process. There was also a simple adjustment to the brightness to ensure that the images appeared balanced compared to each other; in particular, to make sure that images did not appear too bright or too dim compared to others. To ensure that the system was not reliant solely upon the fixed pattern, a minor form of data augmentation was applied to the data. This directly consisted of minor rotations, minimal contrast changes, and minimal basic geometric transformations. After all the pre-processing steps had been completed, the data split was done the same way as in previous examples. About eighty percent of the images used in the analysis went to training, while the remaining twenty percent was used for independent testing. There were no patient-derived details isolated from the images, meaning that none of the information was patient-derived or identifiable in nature.

3.2 Problem Identification

The kind of imaging done on breasts can run into problems related to motion and different types of noise, which are even found in ultrasound images. If there is even slight movement of the patient being scanned, the picture is bound to get blurred, and thus features of interest are not distinct in the image. All these problems have to be filtered to ensure that features of interest are not lost.

A mammogram image also creates another challenge, especially where the tumor or area of concern is too small or even close in intensity to the surrounding tissues [3]. Such a small area may be very critical in determining if there is a potential disease indication, but it is not always easily recognizable. Contrast enhancement and intensity normalization subsequently gain importance because it is easier to distinguish these areas from others.

Since mammograms are grayscale, their pixel intensity will depend on tissue thickness, exposure levels, and other variables. To address issues related to these variables, various statistical properties, including changes in texture, contrast, or intensity, are analyzed, ensuring that the mammograms can be classified regardless of exposure levels.

3.3 Tool Selection

The work done in this research was conducted using MATLAB. MATLAB provides an array of image processing tools that are quite valuable for dealing with medical images. The software encompasses various procedures such as image format changes, image quality improvement, observation of the process results, and implementation of various analysis procedures [16]. The list of procedures included in MATLAB makes it easier to test and improve every stage of the process without having to develop everything from scratch.

MATLAB is also a common platform for scientific computing, and many labs utilize MATLAB for image and video processing and other technical applications. In addition to its stability and functionality, MATLAB is chosen for the implementation and testing of the proposed approach because many mathematical and technical operations and functionalities have already been incorporated into MATLAB.

3.4 Methodology

The proposed system will involve a two-stage analysis process. The first stage will involve processing mammogram and thermogram images separately to allow for the processing of each type of image according to its unique nature. The initial processing of the images will occur at this stage, including reading, resizing, and formatting the images for analysis. For mammograms, the images will be converted to a standard grayscale format to standardize their size by removing variances that may have been caused by different acquisition parameters.

Figure 2 describes the comprehensive procedure undertaken by the Dual-Stacked Cancer Detection Model (DSCD). It starts with the acquisition of dual-source input data in the form of grayscale mammographic images and thermal images. Both sources are considered separately for the preprocessing steps, followed by noise reduction and standardization of intensity differences to maintain uniformity by resizing the images to the same size. Additionally, for the thermal images, the colorful images are converted into single-channel thermal estimate maps for assessing the intensity variation pertaining to the temperatures.

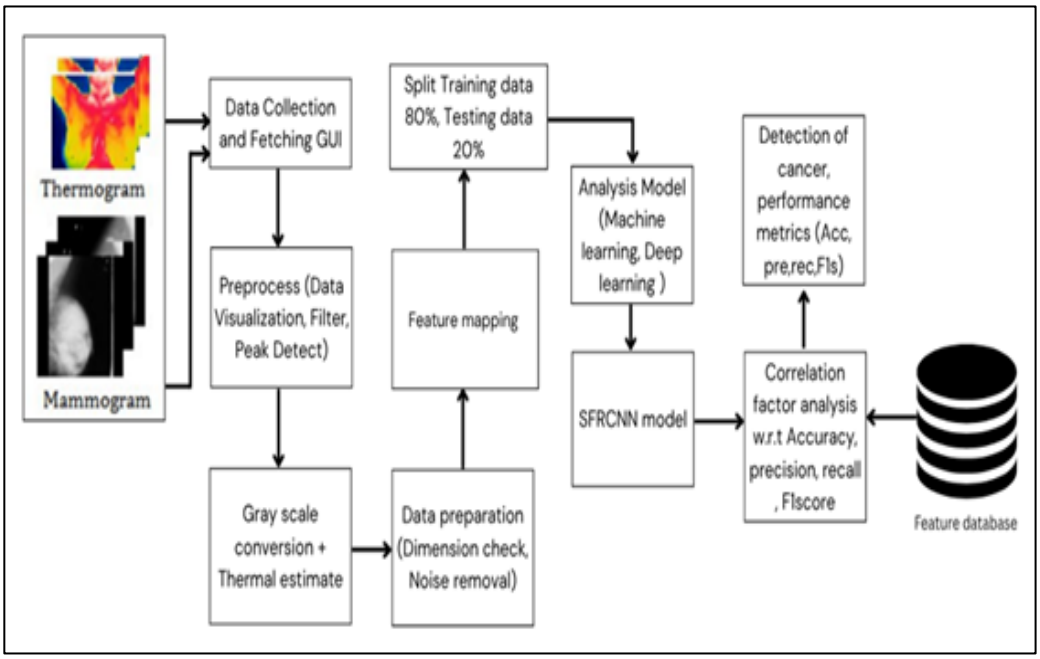

Figure 2. System Architecture of Dual Stacked Cancer Detection Model (DSCD)

Following this processing, a feature extraction process takes place separately for both image streams through a customized ResNet-50-based CNN. The features acquired through the mammogram path and thermogram path are consolidated using a stacked feature fusion technique, which provides a common feature set comprising both structural and thermographic information. The consolidated set of features is then processed through the Super-Fast Recurrent Convolutional Neural Network (SFRCNN) module for final classification. The performance of these predicted classifiers is measured using standard performance criteria such as accuracy, precision, recall, and F1-score. This sequential analysis of processing helps utilize a combination of both modalities for improved levels of breast cancer diagnosis. Multimodal breast cancer diagnosis at a more reliable level has been made possible through this end-to-end processing.

3.4.1 Thermal-Estimate Computation

Thermograms first emerge within a color scale in which every color represents a corresponding temperature. In order for the information to be applicable for calculation, this color scale must be stripped away. Then, every pixel within an image is correlated with its corresponding temperature based on the guide color bar provided within the data set. After this correlation is completed, the thermogram stops acting similarly to an RGB image and begins to function as a temperature sheet.

This temperature map has a similar texture to a gray-scale image. However, the intensity in this map translates to real temperature. To prevent irregular temperature fluctuations due to noise in the sensor and/or small movements of the object of interest, a small amount of smoothing is employed. The result of this processing stage is called the "thermal estimate" and is then passed on to the next stage as input from the "thermal" modality [5], [6], [23].

All these steps make up the data preparation process. After data preparation, a split between training and test data takes place.

3.4.2 Network Selection and Processing Flow

To ensure the analysis is efficient, the proposed framework utilizes a lightweight model rather than the heavy Faster R-CNN-based model. To extract patterns from the modalities, a super-fast recurrent CNN (SFRCNN) is utilized. Its recurrent structure allows for the repeated refinement of information at the pixel level, thus enabling the network to adjust its weights as the image passes through. It is developed based on the ResNet-50 architecture, which has the capacity to extract deep features and retain details by using residual connections, as proposed in [15].

Unlike mammography, in thermography, the process starts with color-coded images. After transformation into thermal estimate maps, standardization follows. All thermal estimates are resized to have equal resolution to ensure they meet the input requirements of the neural network. Variations in resolution could cause variability in interpretation when attempting to combine the feature maps. It is important to perform intensity normalization since every person has different body temperatures. This ensures that neither the bright nor the dull parts are taken to have significant variation and instead relies on form and thermal distribution.

If these preprocessing techniques are integrated, such as removal of color, smoothing of images, resizing of images, and intensity normalization, the resulting thermal images clearly show variations that relate to vascular and/or metabolic processes. The processed images aid the SFRCNN model in detecting detailed patterns in the raw thermal images that are missed when used directly [17].

3.4.3 ResNet-50 Feature Extraction

In the experiment being designed, the modified ResNet-50 architecture is employed as the main feature extractor for the mammogram and thermogram images. The choice of the ResNet-50 model is mainly based on its ability to retain the minute details in medical imagery—edges, contrasts, and various subtle features that tend to get diminished in the later layers of a conventional CNN model. It is thus a prerequisite to detail the processing of the two types of imagery inputs prior to delving into the merging or fusion stage.

The ResNet-50 network is laid out in terms of a series of stages of convolution, where each of the stages progresses based on what the other stages have already learned. In medical images, the details are prone to being washed out as they progress through each of the layers, and the shortcuts used in the ResNet-50 are of great use in passing along such information without washing it out. This is especially important within the context of the current project, where the trace of an abnormality is often seen in the form of faint light or signs of changes in textures, which need to be preserved and then distinguished from the other textures. Figure 3 provides a brief insight into the different steps taken by the altered ResNet-50 model in treating the input images. The images undergo a series of convolutional layers wherein crucial edges and texture information are extracted. The short connections ensure that minute information is retained as the data proceed deeper. Finally, the most useful information is retained and propagated for fusion and classification purposes.

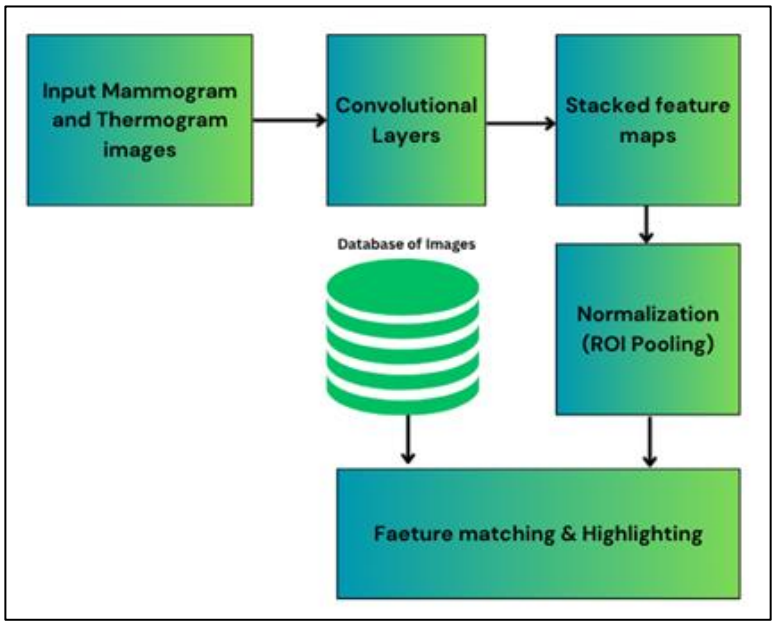

Figure 3. Internal Feature-Extraction Flow of the Customised ResNet-50/SFRCNN Architecture

3.4.3.1 Input Data

The framework accepts two independent inputs: the mammogram $I_M$and the thermal estimate I_T. Both inputs are arranged in a fixed matrix size so that the subsequent layers process them without any dimension mismatch.

3.4.3.2 Feature Extraction using CNN

Each image passes through a dedicated CNN path. For the mammogram, the extractor is denoted as $f_M(\cdot, \theta_M)$, while the thermogram has its own extractor $f_T(\cdot, \theta_T)$. These produce the feature sets:

$$F_M = f_M(I_M, \theta_M), F_T = f_T(I_T, \theta_T) \quad (1)$$

These outputs represent compact descriptions of the structural patterns in the mammograms and the temperature-related variations in the thermal maps.

3.4.3.3 Stacked Feature Fusion

Once the features are extracted, the two outputs are placed next to each other along the channel dimension. This simple stacking keeps the spatial arrangement intact while letting the model view both modalities together:

$$F = \phi([F_M \ || \ F_T]) \quad (2)$$

The operator $\phi(\cdot)$ may be a small dense layer or a light transformation that prepares the fused set for the next stage. This fusion step helps the model relate the edges and textures from the mammogram with the heat-distribution cues from the thermogram.

3.4.3.3 Normalisation/ROI Pooling

If the region-based pooling is applied, then the fused representation is normalised to reduce the local intensity variations:

$$G = Norm\big(\phi(F)\big) \tag{3}$$

This step ensures that the final classifier receives balanced and stable inputs. The choice of ResNet-50 is driven by the nature of the medical images, where the important details often appear as faint boundaries or slight changes in intensity. The skip connections in ResNet-50 allow these early features to pass deeper into the network without being suppressed. This helps the model identify small lesions and weak patterns that a plain CNN might ignore.

Because both modalities become single-channel images after preprocessing, two practical adjustments were made to accommodate ResNet-50. In one approach, the single channel was replicated three times to match the normal RGB input shape. In the other approach, the first convolutional layer of ResNet-50 was modified to accept the single channel directly. Both methods maintain the deeper architecture unchanged, letting the network process the images as usual.

After preprocessing, the feature extraction is given by:

$$FM = ResNet50(I_M) \tag{4}$$

$$FT = ResNet50(I_T) \tag{5}$$

These fused features provide a combined representation that carries both structural and temperature information into the SFRCNN classifier. Because the residual blocks preserve fine-grained cues, the classifier receives clearer signals, especially when dealing with small or low-contrast abnormalities.

3.4.4 Super-Fast RCNN(SFRCNN) Classification Module

The resulting fused features from the two image flows are then analyzed using a Super-Fast RCNN module. For this phase of the research, the thermogram images were provided from the freely available infrared breast thermography database, which has been extensively utilized in many past CNN-based studies for the detection of breast cancer in recent times [20], [17]; For mammograms, cases were provided from the Mammographic Image Analysis Society Database (MIAS) and the Curated Breast Imaging Subset of the Digital Database for Screening Mammography (CBIS-DDSM) public mammography datasets. During testing, each of the images was initially displayed on the computer screen and then processed through the regular procedure until the output reached the SFRCNN level. A small MATLAB interface was utilized in the development phase to validate whether everything worked correctly and to ensure that the output was in sync with what was being delivered in the initial phases.

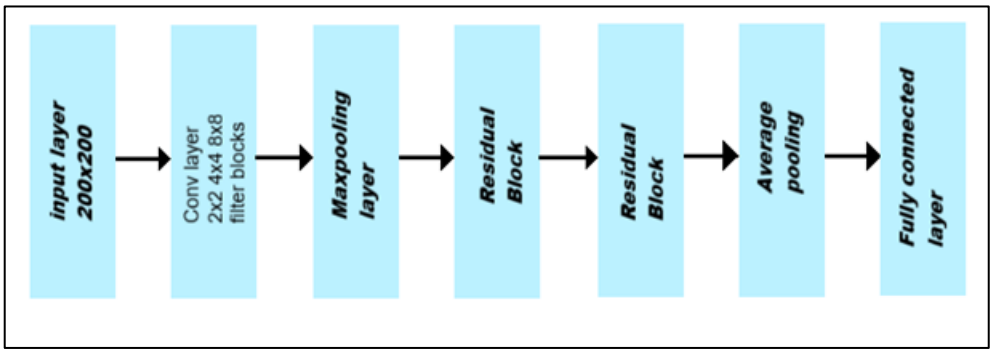

Figure 4. Super-Fast RCNN Architecture

Figure 4 illustrates the SFRCNN block utilized for enhancing the fused features obtained from both streams of mammogram and thermogram images. In this context, the proposed model has been implemented using thermographic images acquired from a public infrared breast thermography image repository, while mammographic images were obtained from the Mammographic Image Analysis Society Database (MIAS) and the Curated Breast Imaging Subset of the Digital Database for Screening Mammography (CBIS-DDSM). In the test phase, each image will be displayed on a monitor, followed by traditional image processing routines. Following these phases, a set of fused features will be processed through an SFRCNN module for classification. Additionally, a simple GUI has been designed in MATLAB to verify whether a set of input images, hidden features, and final outcomes traverse within a traditional flow. The action of convolution layers across the network can be written as:

$$H_t = K(W_c * X_t + b_c) \tag{6}$$

where:

- H_t: feature map at time step t
- W_c: convolutional kernel
- $*$: convolution operation
- b_c: bias
- $K(\cdot)$: activation function (e.g., ReLU)

The fully connected layer gathers the final feature blocks from all samples and helps distinguish between normal and abnormal breast-tissue patterns based on their learned intensity and structural properties.

3.4.4.1 Hyperparameter Tuning and Training Behavior

The SFRCNN configuration also wasn't designed in one go but was achieved over several sessions of tuning on a small scale. Rather than freezing the values of the hyperparameters at the beginning, various patterns for the learning rates had been tried. It was observed that the learning rate at which the loss curve was consistent in going down without sudden peaks or fluctuations was selected for the final phases. The total number of epochs was also not predefined. The training process was allowed to continue only when the accuracy showed a definitive rising pattern and was stopped when the trend started to flatten out.

In the earlier layers, the filter sizes were kept relatively similar to the conventional layout used in ResNet-50. When a few other sizes were tried, the results were more or less the same, and thus there was no particular need to drift away from the original design. Several rounds were conducted in the experiment to check how the model would perform using various combinations of settings, and after monitoring the changes that occurred from one experiment to another in terms of accuracy, loss, and stability, a combination that provided consistent results was taken as the final design for the experiment.

3.4.4.2 Integration with Dual-Modality Streams

After doing the preprocessing, each of these modalities was then fed through its respective path in ResNet-50 so that its individual features could be attended to by the network. This is important because, in mammography, the structural aspects of the image boundaries, patterns of tissues, and shapes are preserved in mammography images, while thermography images capture variations in heat. It is easier for the network to learn contrasts if the features remain separated and do not allow one type of feature to overpower the other.

In turn, it normalized these feature maps in terms of size so that all of them were the same size and could thus be combined into a block. This block contained a combined representation of both the structural cues and the thermal cues. The block, now containing a combined representation of structural cues and thermal cues, was passed through the SFRCNN. Given that it had a repeated structure, it had the capability to revisit those combined features multiple times with the intention of smoothing out the irregular parts.

The last part of the pipeline contains a small dense layer and then a SoftMax layer to output the scores over the classes. In the process of learning, the system would also have gradually learned what the respective patterns normally look like and how the abnormal patterns would differ. Now, given a new input, it weights the input against what it has learned and selects a class based on the appropriate pattern.

3.4.4.3 Rationale for Separate Processing of the Two Modalities

Because each of the two categories of images deals with its own type of information, the first point of handling involves independence. The mammograms would principally illustrate breast tissue structure—bounds, shapes, and tissue distribution—while thermograms would indicate the distribution of heat present on the surface and would generally be associated with variations in blood flow or metabolic rate. After extracting features from both lines of research, these would then be combined by placing them side by side based on the channel axis. This would yield one block that encompasses both the detail of breast structure from the mammogram and the heat distribution from the thermogram. As both sets of information are processed within the same space, it becomes possible to distinguish normal and potentially problematic patterns of breast tissue better with the help of SFRCNN.

4. Results and Discussion

4.1 Thermal Images Under Test

The thermal imaging used for assessment is depicted in Figure 5. These samples underwent an HSV contrast mapping process and an estimation conversion that emphasizes

areas of increased temperature based on thermal intensity. Areas of high intensity have deeper shades of color, while lighter shades correspond to lower intensity. A normal distribution of these would be related to vascular alterations of abnormal tissue activity.

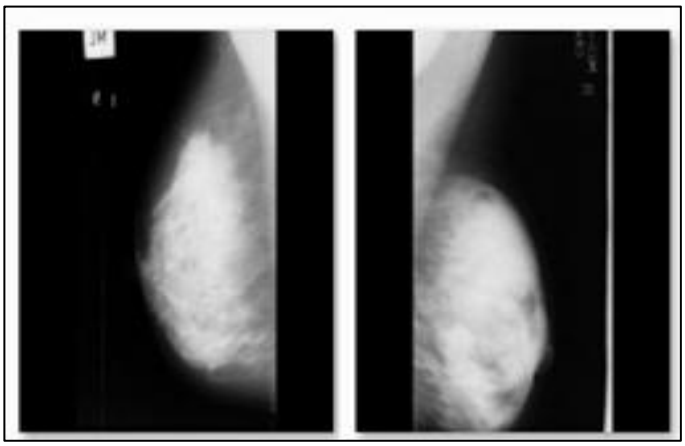

Figure 5. Input Thermal Images Used for Analysis

Before the images are passed into the network, the minute variation due to motion or noise present within the sensors is reduced through the use of light smoothing. Normalization further enhances intensity variation that could be due to uneven heating and background temperatures. Isolated noise points have less effect when the SFRCNN propagates the same fused features repeatedly; thus providing a more representative picture of the tumour-related patterns.

4.2 Mammogram Images Under Test

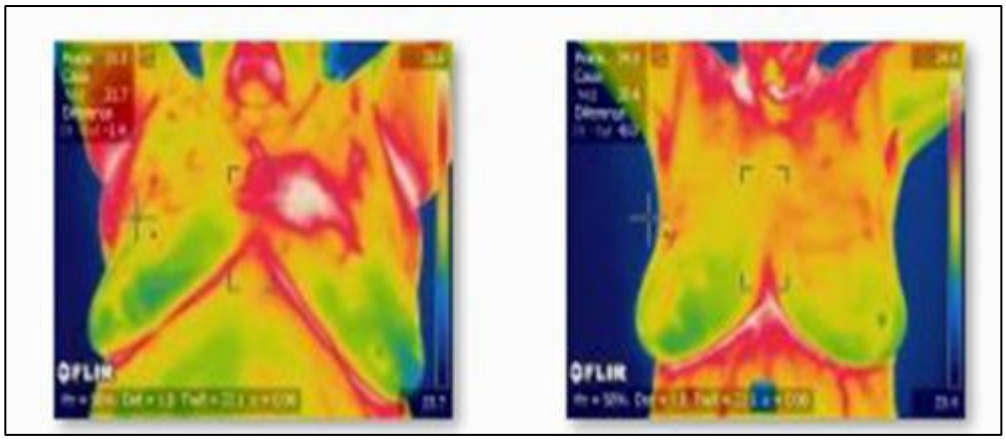

Figure 6. Grayscale Mammogram Images Used for Testing

Figure 6 shows the grayscale image of the mammogram input. The intensity of the input image is usually between 0 and 127, and it is prone to low contrast. During such scanning, the diseased part usually has a higher intensity than its surroundings. In automated analysis, minute differences in intensity are used to identify the diseased areas, although this can sometimes be difficult due to the dense breast tissue.

4.3 Validation of Thermography images

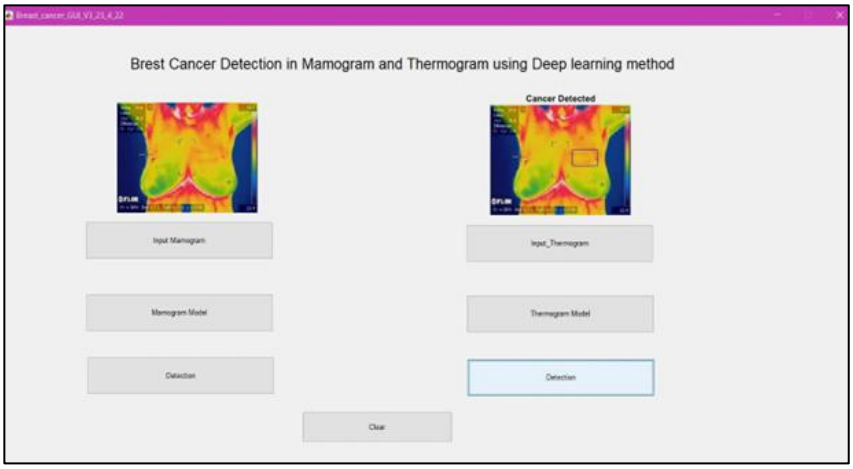

Figure 7. MATLAB Front-End of Thermal Evaluation

Figure 7 displays the MATLAB interface used for validating the thermographic outputs. Generally, the thermal stream managed to locate the abnormal area using the bounding markers obtained based on the changes in temperatures. However, the following samples led to misunderstandings:

- Images showing uniform temperature distributions sometimes imitated vascular activity and caused the model to flag normal areas as suspicious.
- There were instances where the irregularities had poor thermal contrast, making it difficult to identify them among the background patterns.
- Occasionally, slight movement or uneven heating affected the thermal symmetry.

The misclassifications were largely found to occur in borderline or low-contrast cases. This affirms that thermography is very helpful when used along with mammography information, as mammograms offer structural information. [17].

4.4 Validation of Mammograms Images

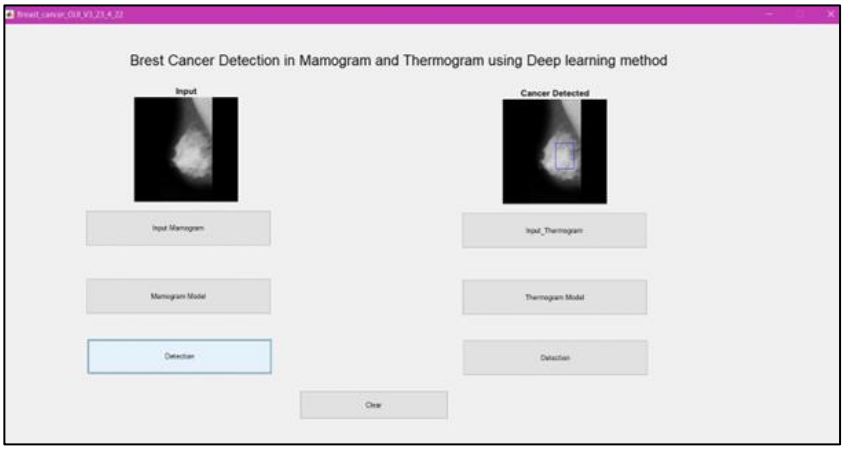

Figure 8. MATLAB Front-End ff Mammogram Evaluation

Figure 8 shows the mammogram-evaluation interface used during testing.The images may also exhibit overlapping regions of tissue that may appear similar to tumors. Dense regions or soft tissues may cause the algorithm to misclassify non-suspicious regions as suspicious. Inhomogeneities in exposure, compression, and illumination are also responsible for false alarms.

These reasons can account for why there were more false positives from the mammogram-based method compared to the thermogram method.

4.5 Comparative Evaluation of Test Images

Table 1. Comparison of TP, FP, FN for Mammogram and Thermogram Images

Metric	Mammogram	Thermogram
TP	250	250
FP	12	3
FN	45	5

These thermal images provide a clear indication of fewer false detections of malignancies, as well as fewer missed malignancies, present within Fig.10.12. These will substantiate the enhanced sensitivity of the thermal patterns.

4.6 True Positive Rate Comparison

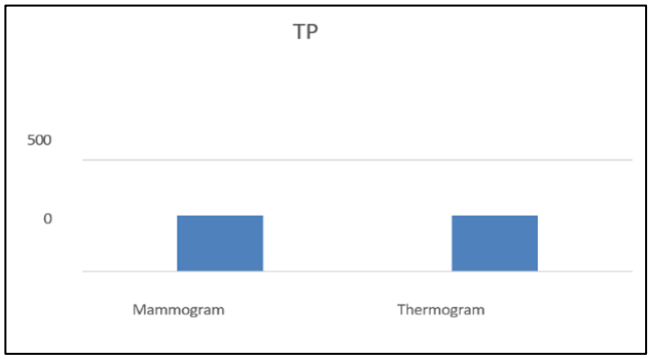

Figure 9. Comparison of True Positive rates of Mammogram and Thermogram

Figure 9 plots a comparison of the true positive rates for mammography and thermography analysis based on the values in table 1.

The thermograms are able to identify 250 out of 255 abnormal patterns (85% TPR). The errors in mammographic images are largely due to tissue overlap and low-contrast lesions.

4.7 False Positives and False Negatives

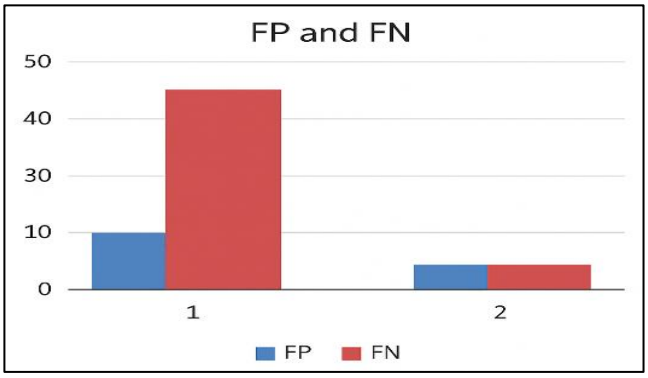

Figure 10. False Positive and False Negative Comparison

Figure 10 illustrates the FP and FN comparison. High FP values are observed in mammograms in cases of dense or overlapping tissues. High FN values are seen in mammograms in situations where the contrast is low for observing the lesions [17].

4.8 Accuracy, Precision, Recall and F1-Score

Table 2. Performance Comparison (Mammogram vs. Thermogram)

Category	Accuracy	Precision	Recall	F1-Score
Mammogram	84.75	95.42	89.23	86.23
Thermogram	98.04	98.81	89.99	92.33

Thermography shows higher accuracy and precision due to the clearer visibility of vascular-heat patterns. Mammograms show higher false positives due to structural ambiguity.

4.9 Performance Analysis Graph

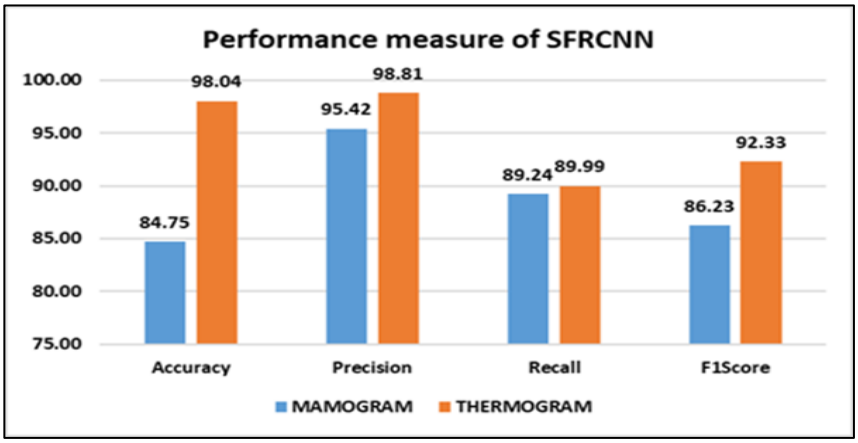

Figure 11. Performance Comparison Graph

Figure 11 presents the accuracy and precision comparison. The combined use of dual modality features significantly improves the overall stability and reduces error likelihood, especially when both structural and thermal cues align.

4.10 Comparison with Conventional CNN

Table 3. Comparison with Conventional CNN and SFRCNN

Method	Image Type	Accuracy	Precision	Recall	F1-Score
Conventional CNN	Mammogram	82.22	85.25	84.25	87.36
Proposed SFRCNN	Mammogram	84.75	95.42	89.24	86.23

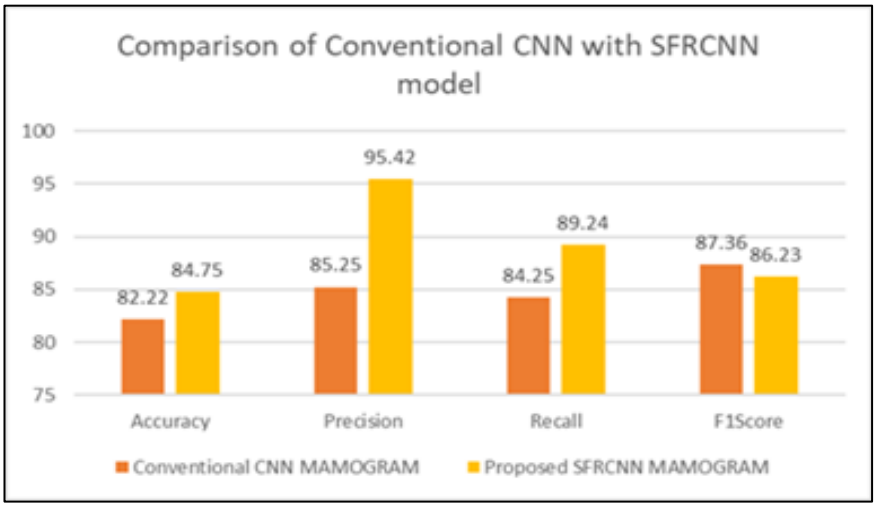

Figure 12. Comparison of Conventional CNN and SFRCNN

4.11 Training and Validation Trends

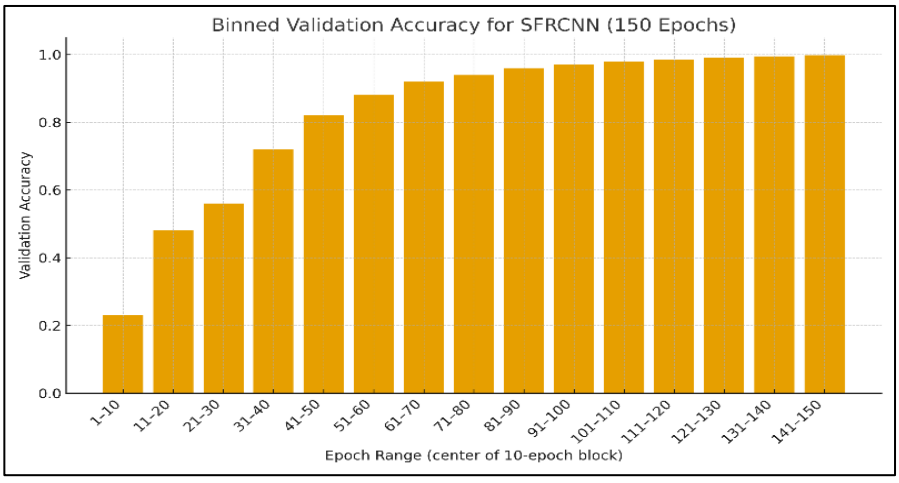

Figure 13. Epoch-Wise Binned Training Loss for 150 Epochs

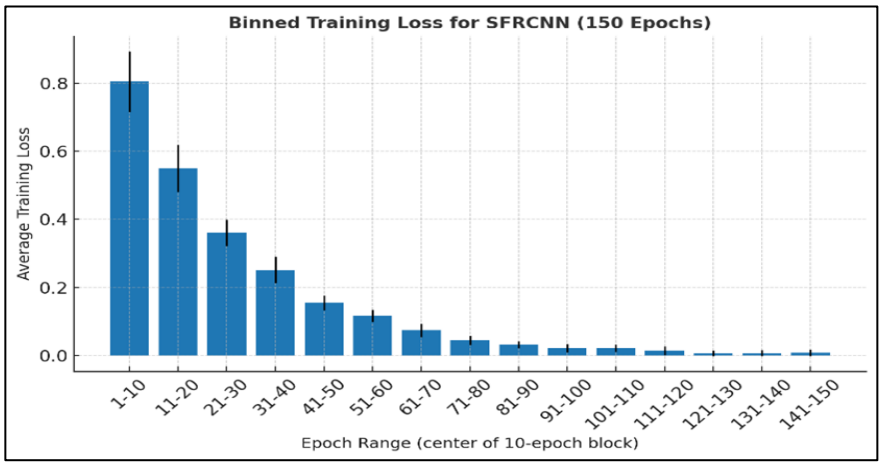

Figure 14. Epoch-Wise Binned Training Accuracy for 150 Epochs

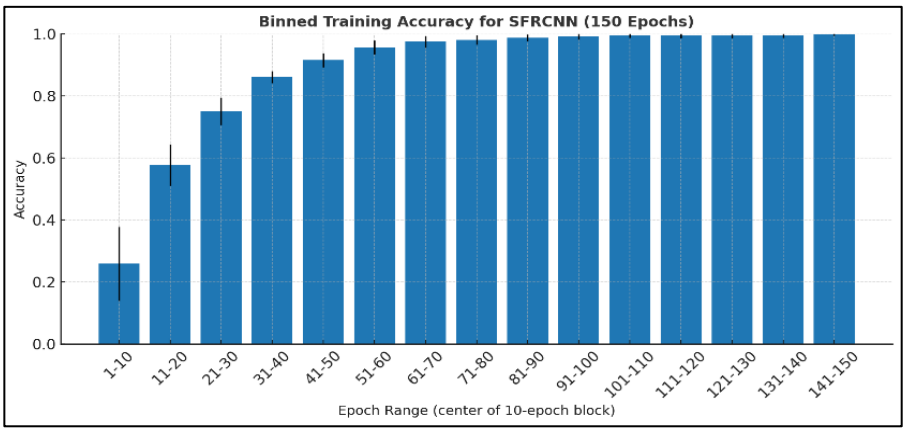

Figure 15. Epoch-Wise Binned Validation Accuracy for 150 Epochs

Figures 13–15 show the training loss, training accuracy, and validation accuracy across epochs. The steady reduction in the training loss and the rise in the accuracy indicate the effective convergence. Validation accuracy stabilizes in the later epochs, showing the improved generalization.

5. Conclusion

With the fusion of images from the mammography system and the thermography system, along with images representing surface temperature, this proposed study confirms the utility of multi-modal fusion in breast cancer imaging. It provides a completely new perspective on tackling this issue because this specific diagnostic solution cannot be attained with the sole use of either system. The proposed approach using SFRCNN would be more accurate. A thorough thermographic analysis was conducted for the patients undergoing exercises, achieving a standard of at least 98.0% true positives with five or fewer false negative values and three or fewer false positives. This indicates a standard level for diagnosis, although due consideration was given to the pathological differences present in whole body temperatures. In the current scenario for analyzing the mammogram, the standard level was maintained at 85.0% true positives with overlapped tissues. The results of the performance assessment indicated that the accuracy of thermograms was 98.04% with an F1 score of 92.33%, while that of

mammograms was 84.75% with an F1 score of 86.23%. It was also ensured that the fusion method performed better than the individual modalities. Thus, there is an improvement in the accuracy of the baseline methods, which was approximately 82.22%. The fusion technique developed on SFRCNN showed better convergence in training and validation, proving its efficiency and effectiveness. Future tasks will involve applying this to more complicated sources of information.

References

[1] Nicolis, Orietta, Denisse De Los Angeles, and Carla Taramasco. "A contemporary Review of Breast Cancer Risk Factors and the Role of Artificial Intelligence." Frontiers in Oncology 14 (2024): 1356014.

[2] R. Sh a, Y. Zhang, L. Wang, X. Li, and Z. Liu, “Global Burden of Breast Cancer and Attributable Risk Factors in Women: New Estimates for 2021,” Biomarker Research, vol. 12, no. 1, 2024, 1–15.

[3] Gilbert, Fiona J., and Katja Pinker-Domenig. "Diagnosis and Staging of Breast Cancer: When and How to Use Mammography, Tomosynthesis, Ultrasound, Contrast-Enhanced Mammography, and Magnetic Resonance Imaging." Diseases of the Chest, Breast, Heart and Vessels 2019-2022: Diagnostic and Interventional Imaging (2019): 155-166.

[4] Abeelh, Enas Abu, and Zain AbuAbeileh. "Comparative Effectiveness of Mammography, Ultrasound, and MRI in the Detection of Breast Carcinoma in Dense Breast Tissue: A Systematic Review." Cureus 16, no. 4 (2024).

[5] Yarabarla, Mamatha Sai, Lakshmi Kavya Ravi, and A. Sivasangari. "Breast Cancer Prediction Via Machine Learning." In 2019 3rd international conference on trends in electronics and informatics (ICOEI), IEEE, 2019, 121-124.

[6] Dabass, Jyoti, Shaveta Arora, Rekha Vig, and Madasu Hanmandlu. "Segmentation Techniques for Breast Cancer Imaging Modalities-A Review." In 2019 9th International Conference on Cloud Computing, Data Science & Engineering (Confluence), IEEE, 2019, 658-663.

[7] Ibrahim, Abdelhameed, Shaimaa Mohammed, Hesham Arafat Ali, and Sherif E. Hussein. "Breast Cancer Segmentation from Thermal Images Based on Chaotic Salp Swarm Algorithm." IEEE Access 8 (2020): 122121-122134.

[8] Robin, Mirya, Jisha John, and Aswathy Ravikumar. "Breast Tumor Segmentation Using U-NET." In 2021 5th international conference on computing methodologies and communication (ICCMC), IEEE, 2021, 1164-1167.

[9] Khasana, Uswatun, Riyanto Sigit, and Heny Yuniarti. "Segmentation of Breast Using Ultrasound Image for Detection Breast Cancer." In 2020 International Electronics Symposium (IES), IEEE, 2020, 584-587.

[10] Nguyen, Thanh-Tam, Thanh-Hai Nguyen, Ba-Viet Ngo, and Duc-Dung Vo. "Breast Image Segmentation for Evaluation of Cancer Disease." In 2020 5th International Conference on Green Technology and Sustainable Development (GTSD), IEEE, 2020, 344-348.

[11] Chavez, Tanny, Nagma Vohra, Jingxian Wu, Magda El-Shenawee, and Keith Bailey. "Spatial Image Segmentation for Breast Cancer Detection in Terahertz Imaging." In 2020 IEEE International Symposium on Antennas and Propagation and North American Radio Science Meeting, IEEE, 2020, 1157-1158.

[12] Georgas, Konstantinos, Ioannis A. Vezakis, Ioannis Kakkos, Anastasia Natalia Douma, Evangelia Panourgias, Lia A. Moulopoulos, and George K. Matsopoulos. "Rad-EfficientNet: Improving Breast MRI Diagnosis Through Integration of Radiomics and Deep Learning." IEEE Journal of Biomedical and Health Informatics (2025).

[13] Al-Antari, Mugahed A., Mohammed A. Al-Masni, Mun-Taek Choi, Seung-Moo Han, and Tae-Seong Kim. "A Fully Integrated Computer-Aided Diagnosis System for Digital X-ray Mammograms Via Deep Learning Detection, Segmentation, And Classification." International journal of medical informatics 117 (2018): 44-54.

[14] Loza, Carlos A. "RobOMP: Robust Variants of Orthogonal Matching Pursuit for Sparse Representations." PeerJ Computer Science 5 (2019): e192.

[15] Khater, Tarek, Abir Hussain, Riyad Bendardaf, Iman M. Talaat, Hissam Tawfik, Sam Ansari, and Soliman Mahmoud. "An Explainable Artificial Intelligence Model for the Classification of Breast Cancer." IEEE Access (2023).

[16] Deng, Tianpeng, Chunwang Huang, Ming Cai, Yu Liu, Min Liu, Jiatai Lin, Zhenwei Shi et al. "FedBCD: Federated Ultrasound Video and Image Joint Learning for Breast Cancer Diagnosis." IEEE Transactions on Medical Imaging (2025).

[17] Jiang, Jiale, Junchuan Peng, Chuting Hu, Wenjing Jian, Xianming Wang, and Weixiang Liu. "Breast Cancer Detection and Classification in Mammogram Using a Three-Stage Deep Learning Framework Based on PAA Algorithm." Artificial Intelligence in Medicine 134 (2022): 102419.

[18] Al-Masni, Mohammed A., Mugahed A. Al-Antari, Jeong-Min Park, Geon Gi, Tae-Yeon Kim, Patricio Rivera, Edwin Valarezo, Mun-Taek Choi, Seung-Moo Han, and Tae-Seog Kim. "Simultaneous Detection and Classification of Breast Masses in Digital Mammograms Via a Deep Learning YOLO-based CAD System." Computer methods and programs in biomedicine 157 (2018): 85-94.

[19] Alzahrani, Riyadh M., Mohamed Yacin Sikkandar, S. Sabarunisha Begum, Ahmed Farag Salem Babetat, Maryam Alhashim, Abdulrahman Alduraywish, N. B. Prakash, and Eddie YK Ng. "Early Breast Cancer Detection Via Infrared Thermography Using a CNN Enhanced with Particle Swarm Optimization." Scientific Reports 15, no. 1 (2025): 25290.

[20] Alshamrani, Khalaf, Hassan A. Alshamrani, Fawaz F. Alqahtani, and Bander S. Almutairi. "Enhancement of Mammographic Images Using Histogram-Based Techniques for Their Classification Using CNN." Sensors 23, no. 1 (2022): 235.

[21] Almalki, Yassir Edrees, Toufique Ahmed Soomro, Muhammad Irfan, Sharifa Khalid Alduraibi, and Ahmed Ali. "Impact of Image Enhancement Module for Analysis of Mammogram Images for Diagnostics of Breast Cancer." Sensors 22, no. 5 (2022): 1868.

[22] Abdelrahman, Leila, Manal Al Ghamdi, Fernando Collado-Mesa, and Mohamed Abdel-Mottaleb. "Convolutional Neural Networks for Breast Cancer Detection in Mammography: A Survey." Computers in biology and medicine 131 (2021): 104248.

[23] Sawyer-Lee, R., Gimenez, F., Hoogi, A., & Rubin, D. (2016). Curated Breast Imaging Subset of Digital Database for Screening Mammography (CBIS-DDSM) [Data set]. The Cancer Imaging Archive. https://doi.org/10.7937/K9/TCIA.2016.7O02S9CY.

[24] https://www.kaggle.com/datasets/kmader/mias-mammography